ELSEVIER

Physica A 291 (2001) 299–316

PHYSICA A

www.elsevier.com/locate/physa

Coupled map lattices with complex order parameter

Sergey P. Kuznetsov[a,*], Erik Mosekilde[b]

[a] *Institute of Radio-Engineering & Electronics, Russian Academy of Sciences, Zelenaya 38, Saratov 410019, Russia*

[b] *Department of Physics, The Technical University of Denmark, 2800 Kgs.Lyngby, Denmark*

Received 16 June 2000

Abstract

We introduce and study coupled map lattices with complex state variable. The dynamical regimes of the finite-length systems are classified naturally in terms of a topological invariant – the overall phase shift accumulated along the whole length at fixed time. A stability analysis of the spatially uniform states is presented, and the results of numerical simulations of the spatio-temporal dynamics are discussed. We demonstrate that fast amplitude evolution, including regular and chaotic spatio-temporal behavior, takes place on the background of a slower phase evolution. For large values of the topological invariant the phase dynamics may give rise to an instability, which in some cases results in a jump of the system to another value of the invariant. We also consider the formation of long-lived "bubbles", i.e., local domains of complicated dynamics in the spatial regions of locally reduced phase gradient. Our coupled map lattice model and its generalizations may be useful for understanding the dynamics in a larger range of parameters for such nonlinear dissipative media, which allow small-amplitude description in terms of the complex Ginzburg–Landau equation, as well as for time-delay feedback systems with nonzero central frequency of the generated signal.

PACS: 05.45.Ra; 05.45.Xt; 05.45.−a; 63.90.+t

Keywords: Coupled maps; Order parameter; Extended systems; Spatio-temporal dynamics

1. Introduction

Coupled map lattices (CML) were introduced in the mid-1980s as a simple and convenient class of models for complicated spatio-temporal dynamics in terms of discrete space and time [1–14]. The CML may be thought as a spatially ordered set of cells

* Corresponding author.
E-mail address: kuz@spkuz.saratov.su (S.P. Kuznetsov).

0378-4371/01/$ - see front matter
PII: S0378-4371(00)00506-9

where the states of the cells are characterized by a continuous variable updated at each step of the discrete time. It is assumed that the new state of each site depends not only on the previous value of the variable at the same cell, but also on the values for several neighboring sites. Postulating a particular type of dynamics for the individual cells (say, the period-doubling behavior) one can study the CML to understand various peculiarities of regular and chaotic dynamics for a certain class of spatially extended systems. An extensive list of phenomena demonstrated by lattices of period-doubling maps may be found, for instance, in the well-known work of Kaneko [7]: formation of frozen domains, pattern competition, birth, death, and Brownian motion of defects, defect turbulence, and developed spatio-temporal chaos. Many successful applications of CMLs are known for concrete systems in physics, chemistry, and biology [15–19], and the theoretical analysis of CMLs has stimulated a number of experimental works aimed at realizing the corresponding phenomena in electronic and other systems [20–23].

It is customary to apply the term *order parameter* when referring to the dynamical variable that represents the states of the cells. This term is adopted from the theory of phase transitions; in general, the order parameter is regarded as a locally defined macroscopic characteristic of a medium, which may depend on spatial coordinates and evolve in time. Numerous examples are known of equations, either derived from the first principles or constructed artificially, which describe spatio-temporal evolution of the order parameter in specific cases [24].

The order parameter may be not only a scalar, but a vector variable as well. One typical example relates to a situation when the spatially uniform state of some medium loses stability in a narrow interval of wave numbers and frequencies. Then, under very general circumstances the spatio-temporal evolution of complex amplitude is governed by the well-known Ginzburg–Landau equation [24–27]. For the case of one spatial dimension it reads as

$$\partial Z/\partial t = AZ - b|Z|^2 Z + D\partial^2 Z/\partial x^2 \,, \tag{1}$$

where A, b, and D are constant coefficients (in general, complex). The order parameter here is the complex variable $Z = Z(x, t)$, which represents the slow amplitude of the evolving perturbation. Note the symmetry property of Eq. (1): It is invariant under a phase shift, i.e., with respect to the variable change $Z \to Ze^{i\phi}$, where ϕ is an arbitrary constant.

In numerous studies devoted to CML only the case of scalar order parameter has been considered in detail. Let us present a simple example demonstrating that sometimes this is not sufficient. Suppose we have a lattice (or a continuous medium) that consists of elements (building blocks) with dynamics governed by an *autonomous* low-dimensional system with *continuous* time (see e.g. [28,29]). Let us assume that with the help of the Poincaré section method we can, with good approximation, reduce the dynamics of an individual element to a one-dimensional map. Does it mean that the lattice of such coupled maps will represent the lattice (medium) under study? In general no: As we consider not one element, but a set of elements, we should account for the possibility

that they have different times of crossing the surface of the Poincaré section. This must be described as the presence of some phase shift between the elements.

In this way, we come to the idea of attributing an additional variable – a phase to the cells of the CML, and to turn to lattice models with complex order parameter. Such models may be regarded as analogs of the Ginzburg–Landau equation, but with discrete space and time. We expect that they will be useful for understanding the dynamics in a larger range of parameters for media, which allow small-amplitude description in terms of the Ginzburg–Landau equation.

CML with complex order parameter are also of interest in the context of delay-feedback systems. As known, a kind of space-time analogy is valid for such systems: they appear to be very close to CML in their dynamical behavior [30–33]. Suppose we have a device containing an amplifier and a narrow-band frequency filter in the loop of delayed feedback. Let the signal circulating in the loop have some central frequency ω_0 and a bandwidth $\Delta\omega$, and assume that $\omega_0 \gg \Delta\omega \gg T^{-1}$, where T is the time delay [30]. In this case one may describe the signal in terms of complex amplitude which has a slow time dependence on the time scale ω_0^{-1}. This amplitude will serve as the complex order parameter for the CML model of the system. The dependence of the complex amplitude on time in one interval of the delay is an analog of the spatial distribution of the order parameter. Each new interval of duration T corresponds to the next step of discrete time evolution in terms of the CML model.

The aim of this paper is to introduce and study the simplest version of coupled map lattices with complex order parameter. Namely, we consider lattices with the dissipative type of coupling. This means that the coupling is of such a nature that it tends to equalize the states of the interacting elements. Nevertheless, we shall see that this model demonstrates a rather rich and complicated dynamical behavior.

The paper is organized as follows. In Section 2, we formulate the dynamical equations for a lattice of maps with complex variable and dissipative coupling of the cells. In Section 3, we consider qualitative peculiarities of the spatio-temporal dynamics associated with the complex nature of the order parameter. In particular, for a lattice with periodic boundary conditions we introduce the concept of topological phase invariant, and we outline the process of long-term phase relaxation. In Section 4, we consider spatially uniform states of the model and analyze their stability. In Section 5, the results of numerical simulations of the spatio-temporal dynamics are presented and discussed. Finally, the conclusion gives a resume of our results and an overview of some possible directions of further studies.

2. Basic equations

Let us start with a discrete-space analog of the one-dimensional Ginzburg–Landau medium:

$$\partial Z_k/\partial t = AZ_k - b|Z_k|^2 Z_k + D(Z_{k-1} - 2Z_k + Z_{k+1})\,, \tag{2}$$

where k designates the spatial index. This may be regarded as a set of coupled elements. In isolation, each element is governed by the equation

$$\partial Z/\partial t = AZ - b|Z|^2 Z \,. \tag{3}$$

Let us try to modify the last relation. We introduce a discrete rather than a continuous time and define the dynamics of the single element by the following complex map:

$$Z_{n+1} - Z_n = AZ_n - b|Z_n|^2 Z_n \quad \text{or} \quad Z_{n+1} = aZ_n - b|Z_n|^2 Z_n \,, \tag{4}$$

where n is the discrete time, and $a = 1 + A$. Without loss of generality, the parameter a may be taken to be real (this corresponds to a proper selection of the central frequency when we define the complex amplitude Z for the process under consideration). Parameter b may be complex. The sign of the real part of b determines whether the nonlinearity suppresses (Re $b > 0$) or supports (Re $b < 0$) the growth of perturbations. The imaginary part reflects the nonlinear influence of the amplitude on the phase. In the present study we restrict our consideration to the case of real positive b; using an appropriate normalization for Z we can set $b = a$.

The map (4) has a trivial fixed point at the origin, $Z = 0$. This point becomes unstable starting from $a_0 = 1$, which corresponds to a symmetry-breaking bifurcation: a circle consisting of fixed points appears. The fixed points are stable with respect to amplitude perturbations and are of neutral stability with respect to a phase shift. For nonzero solutions we can substitute $Z = Re^{i\varphi}$ and hence arrive at a real one-dimensional map for the amplitude:

$$R_{n+1} = aR_n(1 - R_n^2) \tag{5}$$

and a trivial map for the phase

$$\varphi_{n+1} = \varphi_n \,. \tag{6}$$

The nonzero fixed point $R = \sqrt{1 - 1/a}$ existing for $a > a_0$ loses its stability at $a_1 = 2$, when a period-2 cycle appears. Hereafter, a period-doubling sequence follows, with bifurcation values of

$$a_2 = 2.2360679\ldots, \quad a_3 = 2.2880317\ldots, \quad a_4 = 2.2992279\ldots,$$
$$a_5 = 2.3016289\ldots \tag{7}$$

This sequence converges to the Feigenbaum accumulation point [34,35], $a_c = 2.3022834627\ldots$, – the border of chaos. Note that up to $a = a_* = 3$ iterations which started near the origin never diverge to infinity.

Now we are ready to build a chain of coupled elements. There are different ways to define coupling between neighboring cells: see Refs. [36–39] for a discussion of this matter for lattices with scalar order parameter. In the present paper we choose a special type of coupling, which has been found to exhibit the simplest dynamics in the scalar case (see e.g. [6,7,40,41]). Its distinguishing property is that it tends to equalize the states of the interacting cells. According to the terminology of the papers [6,36,37,41] it is called *the dissipative coupling*. Let us suppose that one-step evolution of the chain

of elements (4) consists of two stages: (i) each element evolves according to Eq. (4) independent of the others and (ii) a new updated Z attributed to each site is obtained from some averaging over the previous states of the neighboring elements. One simple version of such a dissipatively coupled map lattice looks like

$$Z_{n+1,\,k} = \tilde{Z}_{n,\,k} + \varepsilon(\tilde{Z}_{n,\,k-1} - 2\tilde{Z}_{n,\,k} + \tilde{Z}_{n,\,k+1}), \quad \tilde{Z}_{n,\,k} = aZ_{n,\,k}(1 - |Z_{n,\,k}|^2)\,, \qquad (8)$$

where k and n are the space and time index, respectively, and ε is the coupling constant. A slightly more sophisticated version is represented by the equation

$$Z_{n+1,\,k} = aZ_{n,\,k}(1 - |Z_{n,\,k}|^2) + \varepsilon(Z_{n+1,\,k-1} - 2Z_{n+1,\,k} + Z_{n+1,\,k+1})\,. \qquad (9)$$

This applies to the so-called 'future coupling' (see [6,40,41] for discussion of the scalar case).

The disadvantage of the simple Eq. (8) is that it allows only a restricted interval for the coupling parameter ε; for large values of ε divergence occurs. In contrast, in Eq. (9) one can choose an arbitrary, positive ε: the larger ε is the stronger the equalizing action will be of the coupling onto the states of the interacting cells. However, in this case to perform one time step and to find the updated set of Z one needs to solve a set of linear algebraic equations. Due to the three-diagonal structure of the associated matrix, this may be done with the help of a simple standard algorithm [42]. Hence, we prefer the model (9).

It is worth noting that in the case of large coupling, neighboring sites of the lattice (9) inevitably have very close states at the same moment, so there exists a well-defined continuum limit. Namely, we can regard Z as a function of a continuous spatial coordinate x and substitute the second spatial derivative $\partial^2 Z_{n+1}(x)/\partial x^2$ instead of the finite-difference combination presented in Eq. (9). This yields

$$Z_{n+1}(x) = aZ_n(x)(1 - |Z_n(x)|^2) + \varepsilon\partial^2 Z_{n+1}(x)/\partial x^2\,. \qquad (10)$$

3. Qualitative peculiarities of spatio-temporal dynamics

We will assume that the lattice is of finite length L, i.e., $0 \leqslant k < L$, and impose periodic boundary conditions such that $Z_L = Z_0$. The system has yet an intrinsic space scale associated with the characteristic coupling length defined as $l \sim \sqrt{\varepsilon}$. It is natural to suppose that $L/l \gg 1$, and this is also a condition for the spatially extended nature of the model to be of relevance.

Note that both Eqs. (8) and (9) allow for a class of real solutions, $Z_{n,\,k} \equiv \mathrm{Re}\, Z_{n,\,k} \equiv R_{n,\,k}$. In this case the system behaves as a conventional CML with scalar order parameter constructed from period-doubling elements (see e.g. [7,10,11,40,41]). We are interested, however, mainly in the case of complex solutions.

Let us suppose that at some fixed moment of time we have a distribution of the complex amplitude Z changing slowly in space from site to site of the lattice in such a way that it may be regarded as quasi-continuous. In the complex plane of Z this will be represented by some curve; as a consequence of the periodic boundary conditions,

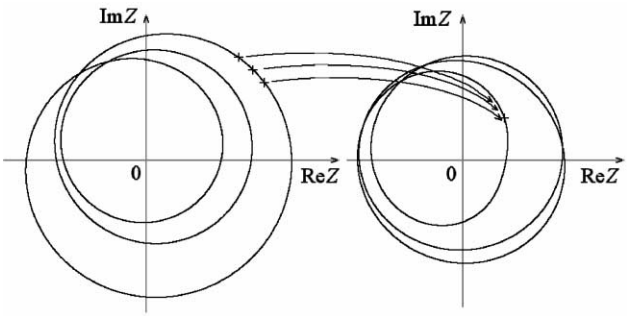

Fig. 1. Definition of the topological invariant: The closed curve on the left plot represents the graph of the complex order parameter as the spatial coordinate is changed over the whole system length at fixed time step. The right plot relates to the next time step. The arrows show schematically the domain of influence of the lattice sites onto the state of some particular cell. The number of excursions around the origin is the topological invariant m.

this curve must be closed (Fig. 1). Suppose that the curve does not contain the origin and does not pass too close to it. Then, there is a well-defined number

$$m = (2\pi)^{-1} \sum_{k=1}^{L} \Delta\varphi_k \,, \tag{11}$$

the phase change for Z accumulated around the curve and measured in units of 2π. It is easy to see that under very general circumstances this value will remain the same after a time step and, hence, may be regarded as a topological invariant. Indeed, at the stage of local nonlinear evolution (i), the direction of vector Z at each site remains unchanged so the accumulated phase shift is conserved. At the stage of coupling (ii) the neighboring sites to a particular cell possess similar complex amplitudes. As the updated amplitude appears as a result of an averaging, it will have approximately the same direction as the original one. Obviously, if we perform one excursion around the whole loop of the original plot we get the same number of rounds in the plane of the updated amplitudes (Fig. 1). The only possibility of a change of the topological invariant in the process of the time evolution is either a passage of the Z-loop across the origin, or the appearance of a fast oscillating spatial pattern. With these exceptions, all dynamical regimes of the system of nonzero amplitude are naturally subdivided into a number of classes, each of which is characterized by a definite value of the topological phase invariant m.

The matter of relevance for our model is the question concerning the evolution of the phase. Let us suppose for a while that we operate in a dynamical regime for which the amplitude $R = |Z|$ remains approximately constant over the whole lattice. (This is possible if we are near the stable fixed point of the individual map (5), $R = \sqrt{1 - 1/a}$.) Then, it is easy to conclude that in the continuum limit the phase $\varphi(x, t)$ will obey the diffusion equation

$$\partial\varphi/\partial t = \varepsilon\partial^2\varphi/\partial x^2 \,, \tag{12}$$

where t denotes continuous time, and x is a spatial coordinate introduced instead of index k. Indeed, substituting $Z = Re^{i\varphi}$ and $\partial^2 Z/\partial x^2 = [R'' + 2iR'\varphi' + iR\varphi'' - R(\varphi')^2]e^{i\varphi}$ into (10) we obtain

$$R_{n+1} + \varepsilon(R''_{n+1} + 2iR'_{n+1}\varphi'_{n+1} + iR_{n+1}\varphi''_{n+1} - R_{n+1}(\varphi'_{n+1})^2)$$

$$= aR_n(1 - R_n^2)e^{i(\varphi_n - \varphi_{n+1})}\,, \tag{13}$$

where the primes designate the spatial derivatives. Neglecting variations of the real amplitude (i.e., $R_n \cong R_{n+1} \cong \sqrt{1 - a^{-1}}$) yields

$$1 - i\varepsilon\partial^2\varphi_{n+1}/\partial x^2 \cong e^{i(\varphi_n - \varphi_{n+1})} \cong 1 + i(\varphi_n - \varphi_{n+1})\,. \tag{14}$$

Finally, changing from discrete time to continuous, we arrive at Eq. (12).

It follows from (12) that the characteristic time of decay of the phase perturbations having the spatial scale Δx must be of order $\Delta t \propto (\Delta x)^2/\varepsilon = (L/l)^2$. The largest spatial scale is the lattice length L, and this corresponds to a time of the phase relaxation $\Delta t \propto L^2/\varepsilon = (L/l)^2$. Considering that $L/l \gg 1$, we notice that this is a very slow process.

If we have a complex amplitude distribution corresponding to the topological invariant m, the boundary condition for the phase equation (12) should be $\varphi|_{x=L} = \varphi|_{x=0} + 2\pi m$. Under this constraint, the final result of the evolution in accordance with Eq. (12) will be a *linear* final distribution of the phase, $\varphi(x) = \varphi_0 + 2\pi mx/L$.

This explains a tendency of linear spatial variations of the phase to arise as observed in the numerical simulations (see Section 5). As it follows from the computations, this phenomenon is intrinsic not only to the states with spatially uniform amplitude distributions, but in some approximation takes place even under more general conditions when nonuniform, nonstationary patterns are present. Also, in these cases the very slow process of the phase evolution is observed, which is of a similar nature to that discussed for the uniform states.

4. Spatially uniform states and their stability

Let us consider in more detail a class of states for our complex CML model characterized by the uniform spatial distribution of the amplitude and a linear phase dependence:

$$Z_{n,k} = R_n e^{i\varphi_{n,k}}, \quad \varphi_{n,k} = \varphi_{n,0} + \gamma k\,, \tag{15}$$

here

$$\gamma = 2\pi m/L \tag{16}$$

is the quantity that we call *the phase gradient parameter*. The last relation ensures consistency of the instantaneous state with the imposed periodic boundary conditions, and it contains an integer m, which is the topological phase invariant. However, in

the asymptotic limit of large L, the dependence of all relevant quantities on γ may be regarded as quasi-continuous.

Substitution of the expressions (15) into the dynamical equation (9) yields

$$[1 + 2\varepsilon(1 - \cos\gamma)]R_{n+1} = aR_n(1 - R_n^2) \tag{17}$$

or

$$R_{n+1} = a'R_n(1 - R_n^2)\,, \tag{18}$$

where

$$a' = a/[1 + 2\varepsilon(1 - \cos\gamma)]\,. \tag{19}$$

The conclusion is that the dynamics of the amplitude in the uniform state is governed by the same equation as the amplitude of an individual element of the CML, but with a reduced parameter a'. Naively, one could think that in the range $1 < a' < 2$ the fixed-point, or period-1 solution would exist as an attractor, and in the ranges $a_{s-1} < a' < a_s$ (see (7)) – cycles of time period 2^s would occur. It appears, however, that stability or instability of these regimes does not depend only on a', but also on the phase gradient parameter γ associated with the topological invariant.

Let us consider a perturbation of the uniform solution and set

$$Z_{n,\,k} = R_n(1 + u_{n,\,k} + \mathrm{i}v_{n,\,k})\mathrm{e}^{\mathrm{i}\gamma k}\,, \tag{20}$$

where $u_{n,\,k}$ and $v_{n,\,k}$ correspond to variations of the amplitude and phase, respectively, and are supposed to be small, $|u_{n,\,k}|$ and $|v_{n,\,k}| \ll 1$. Substituting this expression into (9) we obtain Eq. (18) to zero order, and the equations

$$\begin{aligned} &R_{n+1}[u_{n+1,\,k} - \varepsilon(u_{n+1,\,k+1} - 2u_{n+1,\,k} + u_{n+1,\,k-1})] = aR_n(1 - 3R_n^2)u_{n,\,k}\,,\\ &R_{n+1}[v_{n+1,\,k} - \varepsilon(v_{n+1,\,k+1} - 2v_{n+1,\,k} + v_{n+1,\,k-1})] = aR_n(1 - R_n^2)v_{n,\,k} \end{aligned} \tag{21}$$

in the first order. Now, as usually done in a linear stability analysis, we may search for a solution with a definite wave number, namely, $u_{n,\,k} = U_n\mathrm{e}^{\mathrm{i}\beta k}$ and $v_{n,\,k} = V_n\mathrm{e}^{\mathrm{i}\beta k}$. To simplify the resulting equations we divide them by Eq. (18). This yields

$$\begin{aligned} &\frac{1 + 2\varepsilon(1 - \cos\beta\cos\gamma)}{1 + 2\varepsilon(1 - \cos\gamma)}U_{n+1} + \frac{2\varepsilon\sin\beta\sin\gamma}{1 + 2\varepsilon(1 - \cos\gamma)}\mathrm{i}V_{n+1} = \frac{1 - 3R_n^2}{1 - R_n^2}U_n\,,\\ &-\frac{2\varepsilon\sin\beta\sin\gamma}{1 + 2\varepsilon(1 - \cos\gamma)}\mathrm{i}U_{n+1} + \frac{1 + 2\varepsilon(1 - \cos\beta\cos\gamma)}{1 + 2\varepsilon(1 - \cos\gamma)}V_{n+1} = V_n\,. \end{aligned} \tag{22}$$

Solving this set of two linear equations with respect to U_{n+1} and V_{n+1} we obtain the expression:

$$\begin{bmatrix} U_{n+1} \\ \mathrm{i}V_{n+1} \end{bmatrix} = \mathbf{M}_n \begin{bmatrix} U_n \\ \mathrm{i}V_n \end{bmatrix}\,, \tag{23}$$

where

$$\mathbf{M}_n = \begin{bmatrix} \frac{1-3R_n^2}{1-R_n^2}P(\beta,\,\gamma) & \frac{1-3R_n^2}{1-R_n^2}Q(\beta,\,\gamma) \\ Q(\beta,\,\gamma) & P(\beta,\,\gamma) \end{bmatrix}\,, \tag{24}$$

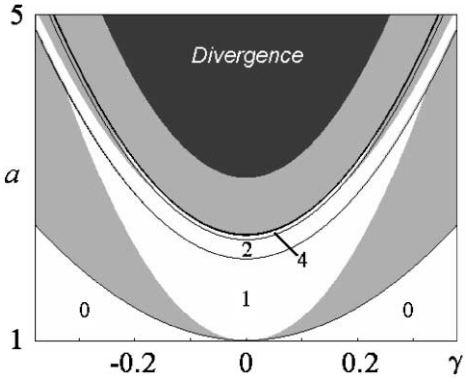

Fig. 2. Parameter plane of nonlinearity parameter a versus phase gradient parameter γ for the CML model (9) at a coupling constant $\varepsilon = 10$. White areas are domains of stability of spatially uniform states, the trivial steady state $R = 0$ is marked by 0, states of nonzero amplitude and of period 1, 2, 4 – by the respective numbers.

with

$$P(\beta, \gamma) = \frac{[1 + 2\varepsilon(1 - \cos\gamma)][1 + 2\varepsilon(1 - \cos\beta\cos\gamma)]}{[1 + 2\varepsilon(1 - \cos(\beta + \gamma))][1 + 2\varepsilon(1 - \cos(\beta - \gamma))]} ,$$

$$Q(\beta, \gamma) = -\frac{2\varepsilon\sin\beta\sin\gamma[1 + 2\varepsilon(1 - \cos\gamma)]}{[1 + 2\varepsilon(1 - \cos(\beta + \gamma))][1 + 2\varepsilon(1 - \cos(\beta - \gamma))]} .$$

Stability of the solution of time period $N = 2^s$ is determined by the eigenvalues μ_1 and μ_2 of the matrix $\mathbf{M}$, which is the product

$$\mathbf{M} = \mathbf{M}_{N-1}\mathbf{M}_{N-2}\cdots\mathbf{M}_1\mathbf{M}_0 . \tag{25}$$

These eigenvalues can be found as the roots of the quadratic equation

$$\mu^2 - S\mu + J = 0 , \tag{26}$$

where S is the trace, and J the determinant of the matrix $\mathbf{M}$.

At each point of the parameter plane (γ, a) we first estimate the period of the cycle to be analyzed (compute a' according to (19) and see what interval $[a_{s-1}, a_s)$ it relates to). Then, we consider μ_1 and μ_2 in dependence on the wave number β and determine the maximum value of their modulus over the whole interval $0 \leqslant \beta < 2\pi$. If this modulus is larger than 1, then the point (γ, a) relates to a region of instability. It should be noted that for $\beta = 0$ one of the eigenvalues always equals 1: Due to invariance of the system with respect to a phase shift, the asymptotically long wave of the phase perturbation possesses a neutral stability – the Goldstone mode [43,24].

In Fig. 2 we present a parameter plane plot where the regions of stability and instability are shown for the spatially uniform states. The states of different time periods are separated by parabola-like curves, namely $a/[1 + 2\varepsilon(1 - \cos\gamma)] = a_s$ (see (7) for the numerical values of a_s). Moving along these curves to the left or to the right, one can observe a loss of stability of the uniform states at some larger values of $|\gamma|$.

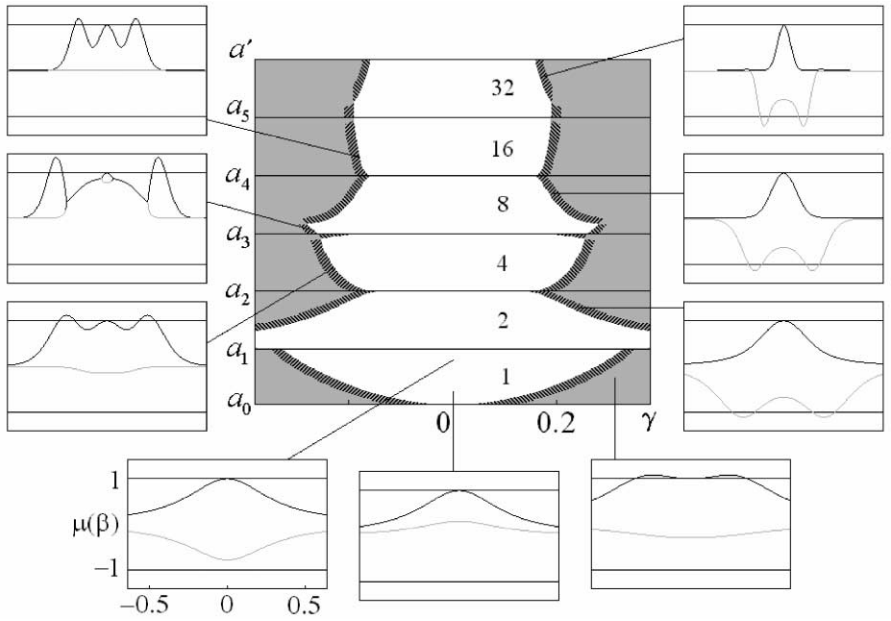

Fig. 3. The middle diagram depicts the parameter plane of nonlinearity parameter a versus phase gradient parameter γ for the CML model (9) at coupling constant $\varepsilon=10$ with a logarithmic scale along the vertical axis (proportional to $\log(a_c - a')$). Numbers $1,\ldots,32$ designate time period of the spatially uniform states inside their stability domains, shown as white. Gray areas correspond to instability. Dashing with two opposite directions designates the stability loss via the eigenvalue equal either to 1, or to -1 at the threshold. The diagrams for eigenvalues versus the wave number are shown at some representative points of the parameter plane around the central figure.

To distinguish the structure of the stability border in more detail we have redrawn the parameter plane diagram in Fig. 3: the parameter of deflection from the critical point of period-doubling accumulation is plotted along the vertical axis in a logarithmic scale. The dashing at the border is of two opposite directions. This corresponds to two distinct situations: one of the eigenvalues becomes equal either to 1, or to -1 at the threshold.

In Fig. 3 we also present a set of plots of eigenvalues versus the wave number at some representative points of the parameter plane. They illustrate the nature of the stability loss at different parts of the stability border. The branch possessing maximum $\mu=1$ at $\beta=0$ may be associated, roughly speaking, with the mode of phase perturbations, and the other branch with the mode of amplitude perturbations. (Of course, only at $\beta = 0$ this classification is exact, otherwise perturbations associated with each branch contain both amplitude and phase oscillations, although in different proportions. In some cases the curves meet, and the eigenvalues become complex. Here it is meaningless to distinguish the amplitude and phase modes.)

The parameter plane region for period 1 has a special arrangement: At the side edges of the stability domain the curve $\mu = \mu(\beta)$, associated with the mode of phase perturbations, displays a maximum of the fourth order. Crossing the boundary leads

to the appearance of three extrema – central minimum at $\beta = 0$, and two symmetric maxima at both sides. The upper boundary is associated with a moment of tangency of the second branch $\mu(\beta)$ with the line $\mu = -1$ at $\beta = 0$.

Surveying the stability domains for higher periods in Fig. 3, one can observe that their structure alternates at subsequent steps of doubling of the time period. For periods $2, 8, 32, \ldots$ the lateral border consists of two notable segments: in one case we have eigenvalue $\mu = -1$ at some wave number β, and in another $\mu(\beta) = +1$. The first situation occurs at the top segment of the boundary; there the instability appears as a growing alternating perturbation of some wavelength. The second case takes place at the bottom part of the boundary and corresponds to the growth of a Turing-like structure without time oscillations. In contrast, for periods $4, 16, 64, \ldots$ the side edges of the stability domain almost entirely relate to an instability of the second kind, $\mu(\beta) = 1$.

5. Numerical simulations

In this section we present results of numerical simulations of spatio-temporal dynamics for our CML model with complex order parameter. It appears useful to treat the computer results in the context of the above linear stability analysis, although they surely go beyond the approximations assumed there.

In the top left corner of Fig. 4 we reproduce the diagram of the parameter plane (γ, a) for $\varepsilon = 10$. The equidistant vertical lines correspond to allowed values of the phase gradient parameter γ associated with integer values of the topological invariant at the lattice length $L = 250$.[1] In the course of our computations a switch from one definite value of the topological invariant to another was produced by multiplying the instantaneous complex amplitudes by $\exp(2\pi i k \Delta m/L)$ at each kth site. Here Δm is an integer, which we wish to add to the topological invariant. Such a redefinition of the instantaneous state of the lattice corresponds to a horizontal jump from one to another of the allowed vertical lines on the plane (γ, a). In this way we could obtain and observe a set of regimes associated with different values of the topological invariant. In fact, they must be regarded as relating to different attractors coexisting in the multidimensional phase space at the same value of the parameter a.

All other plots in Fig. 4 are spatial diagrams, each of which is formed by superimposing instantaneous spatial distributions of the amplitude (solid lines) and of the accumulated phase shift (dotted lines). All the pictures (except the last two) correspond to sustained (at least, approximately sustained) regimes associated with the same nonlinearity parameter a, but with different values of the topological invariant. Observe the different slopes of the phase plots.

For zero γ the presented spatial diagram has been obtained as a final result of the transient process starting from random real initial conditions, $Z_k = R_k$, $0 < R_k < 1$. As

[1] These vertical lines are not continued into the bottom white area of the zero-amplitude state because there the phase is not defined, and the concept of the phase invariance has no sense.

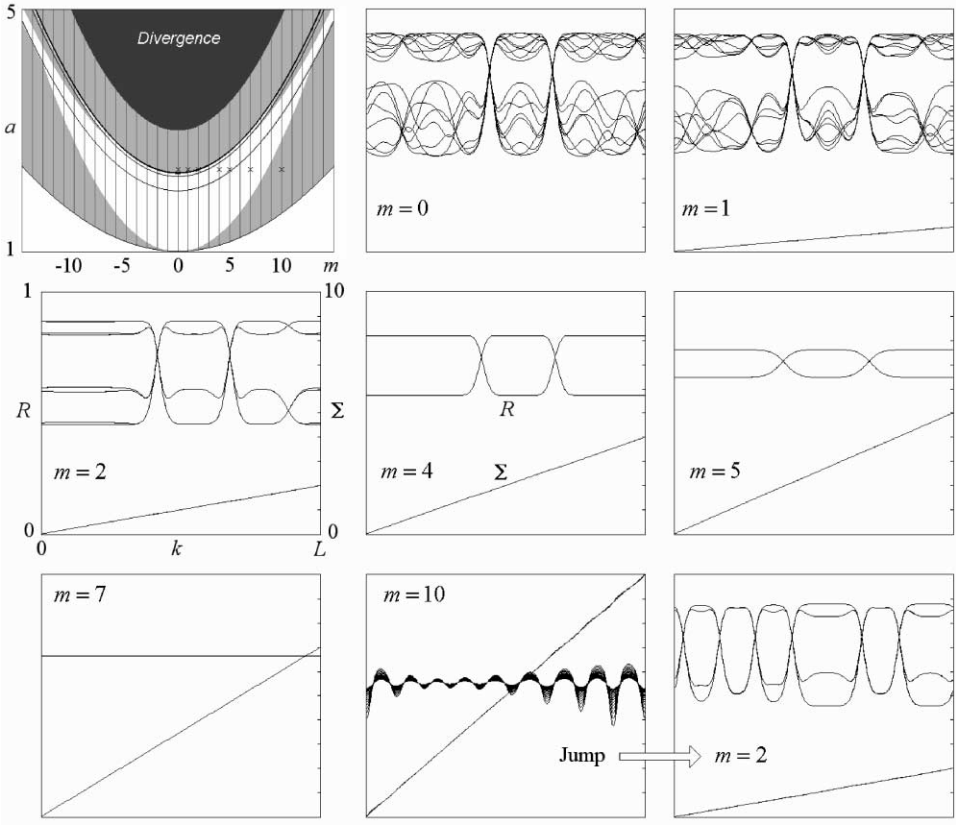

Fig. 4. In the top left corner the parameter plane diagram from Fig. 2 is reproduced. The equi-distant vertical lines correspond to allowed values of the phase gradient parameter, associated with integer values of the topological invariant. The lattice length is $L=250$ and the coupling constant $\varepsilon=10$. All other plots are spatial diagrams, which relate to regimes obtained from the original one ($m=0$) by subsequent switches of the topological invariant, as described in the text. The corresponding points on the parameter plane are marked by small crosses. Each diagram is formed by superposition of 16 instantaneous spatial distributions of the amplitude (solid lines) and of the accumulated phase shift (dotted lines). The last two plots illustrate the development of the phase instability with a jump into the final regime of a reduced value of the topological invariant.

a is slightly larger than the critical value a_c, what is observed is exactly the state called after Kaneko [7] the frozen domain structure. Having local dynamics corresponding to time period $2, 4, 8, \ldots$ we naturally get a number of spatial domains, corresponding to synchronous oscillations of some sets of neighboring cells, separated by the domain walls. The actual lengths of the domains depend on the particular initial conditions. Temporal dynamics inside shorter domains looks more regular, and that inside longer domains looks more chaotic. Moreover, secondary domains, having larger time period of oscillations, may exist inside primary domains of sufficiently large length.

Increasing the topological invariant by subsequent switches $m \to m+1$, as explained above, we observe a transformation of the original domain structure. Although the

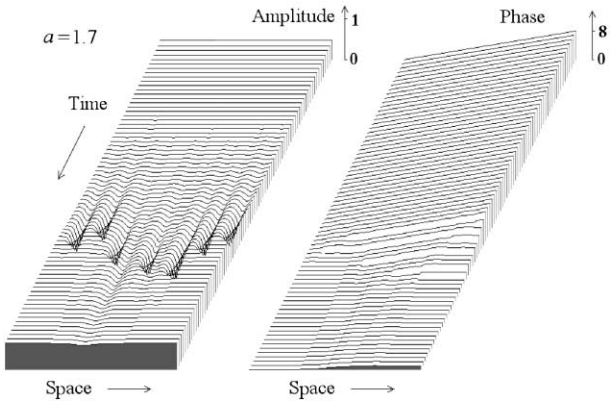

Fig. 5. Space-time diagrams for the amplitude (left) and for the accumulated phase (right) in the model (9), $L=250$, $a=1.7$, $\varepsilon=10$. The initial condition corresponds to a state of constant amplitude, and phase linearly increasing in space (the topological invariant $m=8$); small random perturbations are added. The change of the topological invariant is clearly observed while looking at the right edge of the diagram for phase.

control parameter a is kept constant, we see that the domain structure becomes less developed at larger values of the topological invariant: at $m=2$ the time period 4 is observed inside the domains, at $m=4$ and 5 the period-2 solution is found. At $m=7$ the domain structure vanishes, and the spatially uniform sustained regime takes place. Note that all the regimes are characterized finally by an almost linear dependence of the phase on the spatial coordinate. This agrees with arguments presented in Section 3, although these arguments should be valid, strictly speaking, for states without domains only.

If we increase the topological invariant even more, we finally cross the border of instability for the period-1 homogeneous state and observe a dramatically developing process of growth of perturbations with some dominant wavelength (see the last two plots of Fig. 4). This leads to progressing deflections from the uniform amplitude distribution, and, finally, to a violation of the condition of conservation for the topological invariant. After relaxation of the phase transients the system appears to be in some regime of different, smaller topological invariant. (In the present case this is the regime $m=2$; for other realizations we observed jumps to other values of m as well.) The spatially uniform state of period 1 with this value of the topological invariant belongs to the region of amplitude instability, so the domain structure develops again (see the last plot of Fig. 4).

To relate the dynamics of amplitude and phase in the process of destruction of the topological invariant we present space–time diagrams for amplitude and phase distributions in Fig. 5. They are obtained for $a=1.7$, which corresponds to the regime of sustained time period 1. The initial condition is defined as a state of constant amplitude with the phase linearly increasing in space (the topological invariant $m=8$), and small random perturbations are added. Perturbations of some appropriate wavelength grow

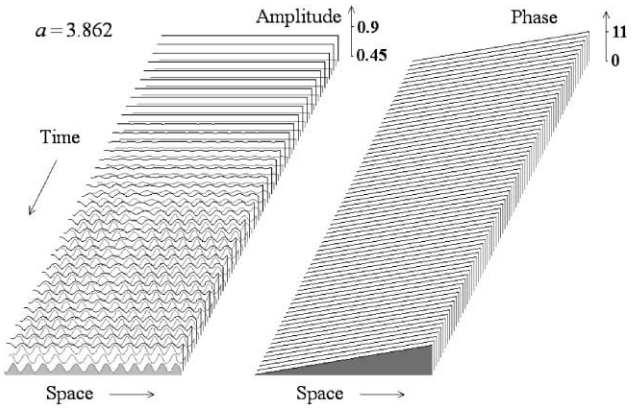

Fig. 6. Same as in Fig. 5, but for $a = 3.862$, $\varepsilon = 10$, $L = 250$. The topological invariant remains constant and equal to the original value $m = 11$ during the whole process.

in time and become visible in the middle part of the diagrams. At some stage of the process they are so large that the amplitude vanishes at some points, and this destroys the topological invariant. After relaxation the system finally appears to be in a regime of smaller topological invariant, in the present case, $m = 1$.

In contrast, development of the phase instability on a background of states of period 2 or higher was observed not to destroy the topological invariant, at least as long as we are not too far from the stability border. In these cases, a kind of pattern formation takes place, see an example in Fig. 6.

As we mentioned in Section 3, one of the essential properties of our system with complex order parameter is a very slow evolution of the phase perturbations, the time scale has been estimated as $T_{\mathrm{ch}} \propto (L/l)^2$. It is worth noting that near the border of the phase instability for the period-1 steady state the phase dynamics becomes yet slower. Indeed, the dependence of the eigenvalue $\mu_1(\beta)$ displays that there is an extremum of the fourth order, so the most long-lived phase perturbations will have characteristic relaxation times of the order $T_{\mathrm{char}} \propto (L/l)^4$.

The final stage of the process of the spontaneous switch of the topological invariant consists typically in this slow phase evolution. If the domain structure is present, it undergoes a slow deformation in the course of this evolution.

Let us turn to one special example and suppose that the initial state of the lengthy CML is prepared in such a way that the value of the local phase gradient depends on the spatial coordinate, being less in some regions and larger in others. As the phase gradient determines the effective value of the nonlinearity parameter a (see (19)), we can observe different regimes of local amplitude dynamics in distinct space intervals. Under appropriate selection of the parameter a we will have long-lived localized "bubbles" of complicated regular or chaotic dynamics separated by domains of steady state. The larger the spatial scales are, the longer the time of existence of the "bubbles" will be. Fig. 7 illustrates this phenomenon. Each diagram shows 16

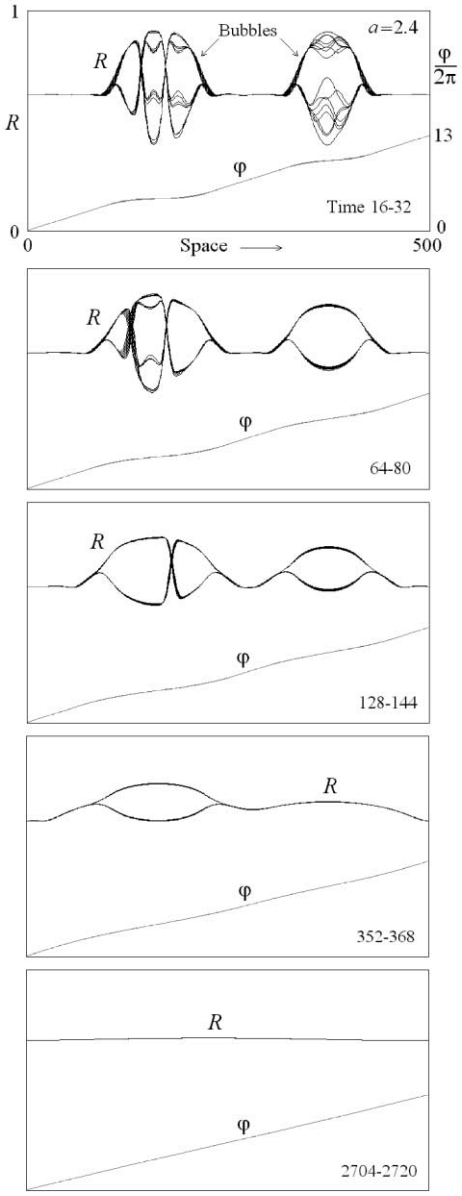

Fig. 7. The spatial diagrams representing superimposed spatial distributions of amplitude and phase at different stages of the slow phase evolution in the model (9), $a=2.4$, $\varepsilon=10$, $L=500$. The initial conditions correspond to random amplitudes in a small range of about $R=0.5$, while the phase dependence on the spatial coordinate has two plateaus. Observe the two "bubbles" which gradually vanish in the course of the slow process of phase relaxation to the linear spatial distribution.

subsequent superimposed spatial distributions of amplitude and phase and belongs to a certain stage of the slow phase evolution. In the initial pictures of Fig. 7 one can see two "bubbles". As the phase distribution gradually relaxes to the linear one, the bubbles vanish. The final stage is the uniform period-1 state with constant phase gradient.

In dependence on the parameter a and on the mean phase gradient γ one can observe either disappearance of the "bubbles" or their coagulation. The whole picture looks similar to a first-order phase transition: the phase gradient plays the role of temperature. Another analogy for the long-lived "bubbles" is well known in hydrodynamics. Here, we refer to the turbulent spots presented in the so-called intermittent turbulence [44–47].

6. Conclusion

As we have asserted in this paper, besides conventional coupled map lattices, which use the scalar state variable, a similar class of models with complex order parameter is of great potential significance. They may be considered as analogs of the Ginzburg–Landau equation with discrete space and time.

We have suggested a concrete CML model with coupling of the dissipative type between the elementary cells, and studied in some detail the peculiarities of its spatio-temporal dynamics. We have argued that the dynamical regimes observed in a finite-length system with periodic boundary conditions are classified naturally in terms of a topological invariant – the overall phase shift accumulated along the system length for fixed time. We have shown that the two components of the dynamical evolution, associated mainly with the amplitude and phase, respectively, possess essentially distinct time scales. Hence, the fast amplitude evolution (that means regular and chaotic spatio-temporal dynamics, pattern formation, competition of patterns, and so forth) develops on a background of slow phase evolution. For some range of values of the topological invariant the phase evolution leads ultimately to almost linear spatial distribution of the phase. Once the system reaches this state, the amplitude regime becomes sustained (at least, in a statistical sense) too. For larger values of the topological invariant the phase dynamics may lead to instability, which in some cases results in violation of the topological invariant and "jumping" to another integer value. For regimes of time period larger than one, the development of the phase instability may not be accompanied by a change of the topological invariant, but results in the emergence of a special kind of spatial pattern. We also emphasize the possibility of formation and evolution of "bubbles" – local domains of complicated dynamics placed in the regions of locally reduced phase gradient. Transformation of this process at the border of the phase instability resembles a phase transition of the first order. This observation may be of interest for search and explanation of similar phenomena in spatially extended systems of different nature.

It is worth stressing once more that our results relate only to the simplest version of the CML with complex order parameter. Even in the scalar case for coupled

period-doubling elements it was shown that there exist two essentially distinct types of coupling [3,36–39]. The complex equation includes the scalar dynamics as a particular case, and both these types of coupling can be introduced into the model. Hence, one could turn to more complicated CML models, than represented by Eqs. (8) and (9), taking into account inertial coupling too. Moreover, the presence of an additional variable, the phase, opens additional possibilities for the construction of coupling, because it may act, generally speaking, in different manners on the amplitude and on the phase of the coupled elements. Next, one could turn to lattices of two and three spatial dimensions with complex order parameter, which will have, surely, much more nontrivial topological properties of the spatio-temporal dynamics. We hope that this paper will stimulate further researches along these directions.

Acknowledgements

S.K. acknowledges the support from the Danish Natural Science Foundation and from the Russian Foundation of Basic Researches, grant No. 00-02-17509.

References

[1] K. Kaneko, Chaos 2 (1992) 279.
[2] K. Kaneko, Progr. Theor. Phys. 72 (1984) 480.
[3] S.P. Kuznetsov, Sov. Tech. Phys. Lett. 9 (1) (1983) 41.
[4] I. Waller, R. Kapral, Phys. Rev. A 30 (1984) 2047.
[5] R. Kapral, Phys. Rev. A 31 (1985) 3868.
[6] S.P. Kuznetsov, A.S. Pikovsky, Physica D 19 (1986) 384.
[7] K. Kaneko, Physica D 37 (1989) 60.
[8] S.P. Kuznetsov, Chaos Solitons Fractals 2 (1992) 281.
[9] D. Stassinopoulos, P. Alstrom, Phys. Rev. A 45 (1992) 675.
[10] F.H. Willeboordse, Phys. Lett. A 183 (1993) 187.
[11] F.H. Willeboordse, Phys. Rev. E 47 (1993) 1419.
[12] V.N. Belykh, E. Mosekilde, Phys. Rev. E 54 (1996) 3196.
[13] R.E. Amritkar, Physica A 224 (1996) 382.
[14] A. Lemaitre, H.R. Chate, J. Stat. Phys. 96 (1999) 915.
[15] T. Yanagita, K. Kaneko, Physica D 82 (1995) 288.
[16] X.-G. Wu, R. Kapral, Phys. Rev. E 50 (1994) 3560.
[17] K. Kaneko (Ed.), Theory and Application of Coupled Map Lattices, Wiley, New York, 1993.
[18] R.V. Sole, J. Bascompte, Phys. Lett. A 179 (1993) 325.
[19] B.E. Kendall, G.A. Fox, Theor. Popul. Biol. 54 (1998) 11.
[20] V.V. Astakhov, B.P. Bezruchko, V.I. Ponomarenko, E.P. Seleznev. Proceedings of the International Seminar on Nonlinear Circuits and Systems, Moscow, 1992, p. 213.
[21] B.P. Bezruchko, V.Yu. Kamenskii, S.P. Kuznetsov, V.I. Ponomarenko, Sov. Tech. Phys. Lett. 14 (6) (1988) 448.
[22] M. de Castro, V. Pérez-Munuzuri, L.O. Chua, V. Pérez-Villar, Int. J. Bifurcation Chaos 5 (1995) 859.
[23] W. Wang, I.Z. Kiss, J.L. Hudson, Chaos 10 (2000) 248.
[24] M.C. Cross, P.C. Hohenberg, Rev. Mod. Phys. 60 (1993) 851.
[25] H.T. Moon, P. Huerre, L.G. Redekopp, Physica D 7 (1983) 135.
[26] R. Brown, A.L. Fabrikant, M.I. Rabinovich, Phys. Rev. E 47 (1993) 4141.
[27] C.R. Doering, J.D. Gibbon, D.D. Holm, B. Nicolaenko, Nonlinearity 1 (1988) 279.
[28] G. Osipov, A. Pikovsky, M. Rosenblum, J. Kurths, Phys. Rev. E 55 (1997) 2353.

[29] A. Goryachev, R. Kapral, Phys. Rev. E 54 (1996) 5469.
[30] S.P. Kuznetsov, Izvestija vuzov – Radiofizika, 25 (1982) 1364, 1410 (in Russian).
[31] P. Malta, C.G. Ragazzo, Int. J. Bifurc. Chaos 1 (1991) 657.
[32] T. Luzyanina, K. Engelborghs, K. Lust, D. Roose, Int. J. Bifurc. Chaos 7 (1997) 2547.
[33] F.H. Willeboordse, Int. J. Bifurc. Chaos 2 (1992) 721.
[34] M.J. Feigenbaum, J. Stat. Phys. 19 (1978) 25.
[35] M.J. Feigenbaum, J. Stat. Phys. 21 (1979) 669.
[36] S.P. Kuznetsov, Radiophys Quantum Electron 28 (1985) 681.
[37] S.P. Kuznetsov, Radiophys Quantum Electron 29 (1986) 679.
[38] H. Kook, F.H. Ling, G. Schmidt, Phys. Rev. A 43 (1991) 2700.
[39] S.Y. Kim, H. Kook, Phys. Rev. E 48 (1993) 785.
[40] J.D. Keeler, J.D. Farmer, Physica D 23 (1986) 413.
[41] S.P. Kuznetsov, in: K. Kaneko (Ed.), Theory and Application of Coupled Map Lattices, Wiley, New York, 1993, p. 50.
[42] W.H. Press, S.A. Teukolsky, W.T. Vetterling, B.B. Flannery, Numerical Recipes in C, Cambridge University Press, Cambridge, 1994, pp. 50–55.
[43] A. Sudbery, Quantum Mechanics and the Particles of Nature, Cambridge University Press, Cambridge, 1986.
[44] P. Bergé, Y. Pomeau, C. Vidal, L'Ordre Dans le Chaos, Hermann, Paris, 1988.
[45] Y. Pomeau, P. Manneville, Commun. Math. Phys. 74 (1980) 189.
[46] B.D. Coller, P.J. Holmes, J.L. Lumley, Phys. Fluids 6 (2) (1994) 954.
[47] G. Metcalfe, R.P. Behringer, Int. J. Bifurc. Chaos 3 (1993) 677.